SEC3 Mutations Are Synthetically Lethal With Profilin Mutations and Cause Defects in Diploid-Specific Bud-Site Selection

B. K. Haarer,*,† A. Corbett,‡ Y. Kweon,† A. S. Petzold,* P. Silver‡ and S. S. Brown*

**Department of Anatomy and Cell Biology, University of Michigan, Ann Arbor, Michigan 48109, †Division of Biological Sciences, Department of Zoology, and Institute for Cellular and Molecular Biology, University of Texas, Austin, Texas 78712 and ‡Dana Farber Cancer Institute, Boston, Massachusetts 02115*

Manuscript received January 9, 1996
Accepted for publication July 5, 1996

ABSTRACT

Replacement of the wild-type yeast profilin gene (*PFY1*) with a mutated form (*pfy1-111*) that has codon 72 changed to encode glutamate rather than arginine results in defects similar to, but less severe than, those that result from complete deletion of the profilin gene. We have used a colony color-sectoring assay to identify mutations that cause *pfy1-111*, but not wild-type, cells to be inviable. These profilin synthetic lethal (*psl*) mutations result in various degrees of abnormal growth, morphology, and temperature sensitivity in *PFY1* cells. We have examined *psl1* strains in the most detail. Interestingly, these strains display a diploid-specific defect in bud-site selection; haploid strains bud normally, while homozygous diploid strains show a dramatic increase in random budding. We discovered that *PSL1* is the late secretory gene, *SEC3*, and have found that mutations in several other late secretory genes are also synthetically lethal with *pfy1-111*. Our results are likely to reflect an interdependence between the actin cytoskeleton and secretory processes in directing cell polarity and growth. Moreover, they indicate that the secretory pathway is especially crucial for maintaining budding polarity in diploids.

IN the budding yeast *Saccharomyces cerevisiae*, the actin cytoskeleton plays a major role in maintaining cellular polarity throughout the budding cycle, largely through its essential role in directing secretion to growing regions of the cell (BRETSCHER *et al.* 1994; WELCH *et al.* 1994). Actin in yeast shows a cell cycle-dependent distribution that suggests a relevance to cellular morphogenesis (ADAMS and PRINGLE 1984; KILMARTIN and ADAMS 1984). This localization is dependent upon cell cycle control elements, including the Cdc28 protein kinase and associated cyclins (LEW and REED 1993, 1995). Furthermore, defects in the single yeast actin gene, or in various genes encoding actin-associated proteins, result in morphogenetic abnormalities, including the delocalized secretion of cell wall components and a partial or complete loss of cellular polarity (BRETSCHER *et al.* 1994).

The small actin monomer-binding protein profilin has been shown to be required for proper actin function in both budding (HAARER *et al.* 1990, 1993) and fission (BALASUBRAMANIAN *et al.* 1994) yeasts, as well as in various other organisms (HAUGWITZ *et al.* 1994; VERHEYEN *et al.* 1994). In budding yeast, elimination of profilin function results in delocalized secretion of cell-wall chitin, disruption of normal budding polarity, loss or perturbation of normal actin localization, and the appearance of abnormal actin bars/aggregates within the cell (HAARER *et al.* 1990). *In vitro* studies with profilins from a variety of organisms, including yeast, have demonstrated that profilin can bind to actin and either retard or enhance its rate of polymerization, depending on the experimental conditions (PANTOLONI and CARLIER 1993; SOHN and GOLDSCHMIDT-CLERMONT 1994). Profilin has also been shown to bind phosphatidylinositol 4,5-bisphosphate (PIP_2) and stretches of proline residues (HAARER and BROWN 1990; HAARER *et al.* 1993; SOHN and GOLDSCHMIDT-CLERMONT 1994; OSTRANDER *et al.* 1995). Despite this wealth of *in vitro* biochemical data, profilin's *in vivo* role remains uncertain. One possibility is that profilin could be acting as a negative regulator of actin polymerization by sequestering actin monomers. This view is supported by the *in vivo* observations of BALASUBRAMANIAN *et al.* (1994), MAGDOLEN *et al.* (1993), and HAUGWITZ *et al.* (1994). Alternatively, profilin could be acting as a positive regulator of polymerization, presumably through the enhancement of the rate of nucleotide exchange on the actin monomer or perhaps by aiding in the assembly of actin monomers at the barbed ends of filaments (PANTALONI and CARLIER 1993). A potential role in the enhancement of polymerization is supported by the apparent *in vivo* role of profilin in stimulating the actin-directed motility of *Listeria monocytogenes* (COSSART 1995).

Very little is known about the proteins, other than actin, that interact with profilin. Further, it is not clear how profilin might be responding to cellular signals to help bring about changes in the actin cytoskeleton. The biochemical identification of a profilin-binding complex (MACHESKY *et al.* 1994) indicates that profilin is

Corresponding author: Brian Haarer, Department of Zoology, 219 Patterson Labs, The University of Texas, Austin, TX 78712-1064. E-mail: haarer@mail.utexas.edu

associated with a multi-protein complex. However, it is not clear whether such interactions occur in addition to, or instead of, profilin's interaction with conventional actin. The role of this protein complex in profilin function is unknown, though components of the complex do colocalize with profilin at the cell cortex (MACHESKY *et al.* 1994).

To obtain a better understanding of profilin's role(s) *in vivo* and to better understand its direct and indirect interactions during the performance of these functions, we have turned to a specific genetic screen that identifies mutations that exacerbate the effects of mildly altered profilin alleles in yeast. This screen has yielded such "synthetic lethal" mutations in several genes. We report here the identification of one of these genes as the previously uncloned *SEC3* gene, which is important for protein secretion (NOVICK *et al.* 1980, 1981), thus supporting a role for profilin and actin in polarized secretion in yeast.

MATERIALS AND METHODS

Yeast strains and growth conditions: *Saccharomyces cerevisiae* strains used in this study are listed in Table 1. Cells were generally grown on rich medium YEPD plates (1% yeast extract, 2% bactopeptone, 2% glucose, 1.6% agar), YEP-glycerol plates (YEPD with 2% glycerol instead of glucose), or liquid YM-P (LILLIE and PRINGLE 1980). For transformations and for maintaining plasmid selection, cells were grown on synthetic complete (SC) medium lacking the appropriate supplement or on minimal SD medium with necessary supplements (SHERMAN *et al.* 1986). Unless otherwise indicated, growth of yeast strains was at room temperature (~22°).

DNA manipulations and yeast genetic techniques: Standard procedures were used for recombinant DNA manipulation and *Escherichia coli* transformation (SAMBROOK *et al.* 1989). Yeast transformation was by the lithium acetate procedure (MA *et al.* 1987). Plasmid stability was assayed by growing transformants nonselectively in liquid medium, plating on YEPD, and scoring the resulting colonies for the plasmid-borne selectable marker by restreaking onto the appropriate medium.

DNA sequencing was by the dideoxy method (SANGER *et al.* 1977) using the Sequenase kit (United States Biochemical, Cleveland, OH). Analysis of DNA and predicted protein sequence was performed using the Genetic Computer Group (GCG) sequence analysis package (DEVEREUX *et al.* 1984), including the coiled-coil prediction program of LUPAS *et al.* (1991).

Replacement of the wild-type profilin gene: The wild-type profilin gene (*PFY1*) was replaced with the *pfy1-111* allele (Arg72 to Glu; HAARER *et al.* 1993), as follows. (1) A 4-kbp *Pst*I DNA fragment containing the *LEU2* gene was inserted into the *Pst*I site of plasmid pSK-H (HAARER *et al.* 1990) to create plasmid pSK-HL. (2) A 1375-bp *Bam*HI-*Ssp*I DNA fragment (generated by complete digestion with *Bam*HI and partial digestion with *Ssp*I) containing the entire mutant profilin gene was then cloned into the *Bam*HI and *Sma*I sites of pSK-HL to create plasmid pSK(A-111)35. (3) A 5.85-kbp *Bam*HI-*Hin*dIII fragment containing the *pfy1-111* allele and the *LEU2* gene from this plasmid was used to transform strain (DC5xY388)2D to Leu$^+$. Integration of this DNA fragment, and the associated replacement of wild-type *PFY1* with the *pfy1-111* allele and the *LEU2* gene was confirmed by (1) tetrad analysis to show linkage between the inserted *LEU2* gene and *ADE2*, which is tightly linked to *PFY1*, (2) DNA hybridization (data not shown), and (3) recovery of the mutant allele by gap repair (ROTHSTEIN 1991; see below) and subsequent sequencing to confirm the presence of the *pfy1-111* mutation. The resulting strain was named BHY14.

Synthetic lethal screening: The *ADE3*, *HIS3*, 2μ vector pTSV32 was constructed by inserting a 1.3-kbp *Xho*I-*Bam*HI fragment containing the *HIS3* gene into the *Sal*I and *Nco*I sites of plasmid pTSV31A (provided by M. TIBBETTS; to be described elsewhere). For the fragment and vector preparation, the *Bam*HI and *Nco*I sites were treated with Klenow to create compatible blunt ends before digestion with *Xho*I and *Sal*I, which generate compatible sticky ends. This construction replaces a large portion of the *URA3* gene and part of the polylinker region of pTSV31A with the *HIS3* gene. The entire *PFY1* gene was inserted into the unique *Sma*I site of pTSV32 as a 787-bp *Ssp*I fragment (this includes 119 and 78 bp of upstream and downstream noncoding sequence, respectively) to create plasmid pTSV-PFY. Yeast strain BHY14 was transformed with pTSV-PFY to generate BHY14*. Screening for BHY14* cells that depend on the plasmid-borne *PFY1* gene for viability was performed essentially as described by BENDER and PRINGLE (1991). Screening was performed either in the absence of mutagenesis or after cells were mutagenized by UV irradiation, which resulted in 15–65% killing.

Marker-rescue experiments: To identify the region of *PSL1* that corresponds to the *psl1-1* allele, we performed marker-rescue experiments (see *e.g.*, LILLIE and BROWN 1994). The *psl1-1 ura3* strain NS(14)1 was transformed at permissive temperature with various fragments of the *PSL1* gene (Figure 5A) cloned into the *URA3*-containing plasmids YCp50 or YEp352. Ura$^+$ transformants were screened for growth at 37°. The occurrence of Ts$^+$ papillae in a background of dying cells ("marker rescue") indicated that a given *PSL1* fragment was able to rescue the *psl1-1* mutation by gene conversion (Figure 5A, MR$^+$). The *psl1-1* lesion was found to reside within a ~750-bp region of DNA flanked by *Sst*I and *Nco*I sites (Figure 5A).

Mapping of *PSL1*: The cloned *PSL1* gene hybridized to either chromosome *V* or *VIII*, which were not well resolved in a DNA blot of whole chromosomes (kindly provided by K. CORRADO). Upon probing a grid blot of cosmid clones (kindly provided by L. RILES and M. OLSON), *PSL1* hybridized to a single cosmid clone whose insert is derived from a region very close to the centromere of chromosome *V*. Tetrad analysis of a cross between BHY44 (*psl1*) and TD4 (*trp1*; tightly linked to CEN IV) yielded 14 parental ditype and 18 nonparental ditype (or 32 first-division segregation) and one tetratype (second-division segregation) tetrads, indicating a map distance of ~1.5 cM between *PSL1* and CEN V [using the formula: map distance = (1/2)SDS/total × 100]. The yeast genome project has recently determined the physical distance between *PSL1* and CEN V to be ~15.7 kb.

Gap repair and gene deletions: To confirm the presence of the *pfy1-111* allele in BHY14, we cloned the profilin locus from BHY14 by gap repair (ROTHSTEIN 1991). This was accomplished by linearizing the 2μ, *URA3*-based plasmid PFY-Gap such that one end of the linear DNA fragment contained the 5′ end of *PFY1* through codon 16, and the other end contained a portion of the *LEU2* gene. BHY14 was transformed to Ura$^+$ with this fragment. Plasmids were recovered from these transformants and the profilin coding region was subcloned to pBluescript SK+. Sequence analysis confirmed that BHY14 contains the *pfy1-111* mutation.

In a similar fashion, we cloned the chromosomal region containing the *psl1-1* mutation by transforming strain BHY47 (*psl1-1*, *leu2*) to Leu$^+$ with YEp351(SEC3-SN) that had been linearized with *Xho*I and *Nco*I, and purified by agarose gel

TABLE 1

***S. cerevisiae* strains used in this study**

Strain	Relevant genotype	Source
22AB	*MATa/MATα trp1/trp1 ura3/ura3 leu2/leu2 his3/his3 lys2/lys2*	HAARER *et al.* (1994)
BHY14	*MATα ade2 ade3 ura3 leu2 lys2 his3 pfy1-111:LEU2*	This study
BHY17	*MATα ade2 ade3 ura3 leu2 his3 pfy1-111:LEU2 sec3-101 (psl1-1)* +pTSV-PFY	This study
BHY18	*MATa ade2 ade3 ura3 leu2 his3 pfy1-111:LEU2 sec3-101 (psl1-1)* +pTSV-PFY	This study
BHY21	*MATa ade2 ade3 ura3 leu2 his3 pfy1-111:LEU2 psl2-1* +pTSV-PFY	This study
BHY22	*MATα ade2 ade3 ura3 leu2 his3 pfy1-111:LEU2 psl2-1* +pTSV-PFY	This study
BHY23	*MATα ade2 ade3 ura3 leu2 his3 pfy1-111:LEU2 psl3-1* +pTSV-PFY	This study
BHY24	*MATa ade2 ade3 ura3 leu2 his3 pfy1-111:LEU2 psl3-1* +pTSV-PFY	This study
BHY26	*MATa ade2 ade3 ura3 leu2 his3 pfy1-111:LEU2 psl4-1* +pTSV-PFY	This study
BHY27	*MATα ade2 ade3 ura3 leu2 his3 pfy1-111:LEU2 psl4-1* +pTSV-PFY	This study
BHY33	*MATa ade2 ade3 ura3 leu2 his3 psl2-1*	This study
BHY34	*MATα ade2 ade3 ura3 leu2 his3 psl2-1*	This study
BHY35	*MATa ade2 ade3 ura3 leu2 his3 psl3-1*	This study
BHY36	*MATα ade2 ade3 ura3 leu2 his3 psl3-1*	This study
BHY37	*MATα ade2 ade3 ura3 leu2 his3 psl4-1*	This study
BHY38	*MATa ade2 ade3 ura3 leu2 his3 psl4-1*	This study
BHY43	*MATa ura3 leu2 his3 sec3-101 (psl1-1)*	This study
BHY44	*MATα ura3 leu2 his3 sec3-101 (psl1-1)*	This study
BHY45	*MATα ade2 ade3 ura3 leu2 his3 pfy1-111:LEU2*	This study
BHY46	*MATa ade2 ade3 ura3 leu2 his3 pfy1-111:LEU2*	This study
BHY47	*MATa/MATα ura3/ura3 his3/his3 leu2/leu2 sec3-101 (psl1-1)/sec3-101(psl1-1)*	This study
BHY48	*Mata/MATα ade2/ade2 ade3/ade3 ura3/ura3 leu2/leu2 his3/his3 pfy1-111:LEU2/pfy1-111:LEU2*	This study
BHY51	*MATa ura3 leu2 lys2 his3 trp1 sec3Δ::LEU2*	This study
BHY52	*MATα ura3 leu2 lys2 his3 trp1 sec3Δ::LEU2*	This study
BHY58	*MATa/MATα ade2/ade2 ade3/ade3 ura3/ura3 leu2/leu2 his3/his3 psl3-1/psl3-1*	This study
BHY63	*MATa/MATα ura3/ura3 leu2/leu2 lys2/lys2 his3/his3 trp1/trp1 sec3Δ::LEU2/sec3Δ::LEU2*	This study
DBY1993	*MATα act1-2 ura3-52*	D. BOTSTEIN
DBY1995	*MATα act1-3 his4-619*	D. BOTSTEIN
DBY1999	*MATa act1-3 ura3-52*	D. BOTSTEIN
DBY2018	*MATa act1-2 his4-619*	D. BOSTEIN
DC5a	*MATa leu2 his3 can^R*	J. PRINGLE
DC5α	*MATα leu2 his3*	J. PRINGLE
(DC5xY388)2D	*MATα ade2 ade3 ura3 leu2 lys2 his3*	This study
(DC5xY388)10A	*MATa ade2 ade3 ura3 leu2 his3*	This study
(DC5xY388)13A	*MATa ade2 ade3 ura3 leu2 lys2 his3*	This study
(DC5xY388)2D+13A	*MATa/MATα ade2/ade2 ade3/ade3 ura3/ura3 leu2/leu2 lys2/lys2 his3/his3*	This study
NS(14)1	*MATα ade2 ade3 ura3 leu2 lys2 his3 pfy1-111:LEU2 sec3-101 (psl1-1)*	This study
NS(14)4	*MATα ade2 ade3 ura3 leu2 lys2 his3 pfy1-111:LEU2 psl2-1*	This study
NS(14)8	*MATα ade2 ade3 ura3 leu2 lys2 his3 pfy1-111:LEU2 psl3-1*	This study
NS(14)14	*MATα ade2 ade3 ura3 leu2 lys2 his3 pfy1-111:LEU2 psl4-1*	This study
NS(14)24	*MATα ade2 ade3 ura3 leu2 lys2 his3 pfy1-111:LEU2 psl5-1*	This study
NY3	*MATa sec1-1 ura3-52*	P. NOVICK
NY17	*MATa sec6-4 ura3-52*	P. NOVICK
NY57	*MATa sec9-1 ura3-52*	P. NOVICK
NY61	*MATa sec10-2 ura3-52*	P. NOVICK
NY64	*MATa sec15-1 ura3-52*	P. NOVICK
NY130	*MATa sec2-41 ura3-52*	P. NOVICK
NY402	*MATa sec5-25 ura3-52*	P. NOVICK
NY405	*MATa sec4-8 ura3-52*	P. NOVICK
NY410	*MATa sec8-9 ura3-52*	P. NOVICK
NY431	*MATa sec18-1 ura3-52*	P. NOVICK
NY757	*MATa sec7-1 his4-619*	P. NOVICK
SLY55	*MATa smy1Δ::LEU2 leu2 ura3 his4*	S. LILLIE
SLY56	*MATa leu2 ura3 his4*	S. LILLIE
SLY102	*MATa smy1Δ::URA3 leu2 ura3*	S. LILLIE
SLY219	*MATa/MATα ura3/ura3 leu2/leu2 his4/his4 sec2-70::URA3/sec2-70::URA3*	S. LILLIE
SLY221	*MATa/MATα ura3/ura3 leu2/leu2 his4/his4 SEC+/SEC+*	S. LILLIE
Y388	*MATa ade2 ade3 ura3 leu2 lys2*	A. BENDER
TD4	*MATa his4-519 ura3-52 trp1-289 leu2-3,112*	J. PRINGLE
αsst2	*MATα sst2*	A. BENDER
XMB4a	*MATa bar1*	A. BENDER
YJC0398	*MATα cap2-1::URA3 leu2 ura3*	J. COOPER
YJC0399	*MATa cap2-1::URA3 leu2 ura3*	J. COOPER

electrophoresis. YEp351(SEC3-SN) is a 2μ, *LEU2*-based vector that contains the same insert as YEp352(SEC3-SN) (see Figure 5A). Thus, the repaired plasmid should contain the ~750-bp region between *Sst*I and *Nco*I that was shown by marker rescue experiments to contain the mutated region of *psl1-1* (*sec3-101*). This repaired plasmid was recovered from yeast and the *Sst*I-*Nco*I region was subcloned and sequenced to determine the nucleotide change(s) of the *psl1-1* allele.

A portion of the *SEC3/PSL1* gene was deleted as follows: The 1.2-kb *Xba*I-*Pvu*II and 1.2-kb *Eco*RI fragments (see Figure 5A; the *Eco*RI site in the 3′ noncoding region is not shown) were cloned into the *Xba*I-*Sma*I and *Eco*RI sites, respectively, of pBluescript KS$^-$. A 4-kb *Pst*I fragment containing *LEU2* was then cloned into the *Pst*I site in the linker region between these fragments. The resulting plasmid, pKS-psl1::LEU2 (Figure 5A), was digested with *Xba*I and *Hin*dIII, and the ~6.4-kb fragment containing portions of the 5′ and 3′ coding regions of *SEC3* interrupted by the *LEU2* gene was used to transform the diploid strain 22AB to Leu$^+$. This effectively replaces codons 435–1119 of *SEC3* with the *LEU2* gene (see Figure 5A). The expected gene replacement was confirmed by DNA hybridization (not shown).

Staining and microscopy techniques: Immunofluorescence microscopy, Calcofluor-, and DAPI-staining were performed as described previously (PRINGLE *et al.* 1989; HAARER *et al.* 1990). Bud-site selection was scored in cells having more than one Calcofluor-stained bud scar. Bud-site selection patterns were determined by essentially dividing the ellipsoidal cells into thirds and scoring them as either unipolar (all scars at one pole of the cell only), bipolar (scars at both poles of the cell, but not in the middle), or random (at least one scar not at either pole). Cells were visualized on Leitz Orthoplan or Zeiss Axioplan microscopes; fluorescence photographs were taken with Kodak T-Max 400 film, which was push-processed to ASA 1600. Black and white negatives and color slides were scanned with a Nikon scanner to convert to positive black and white digital format. Contrast adjustment and creation of montages were performed using Adobe Photoshop.

RESULTS

Replacement of the wild-type profilin gene: Deletion of the yeast profilin gene (*PFY1*) results in severe growth abnormalities (HAARER *et al.* 1990). We have previously shown that various altered profilins that have compromised *in vitro* actin-binding or PIP_2-binding activities could suppress the phenotypes caused by the absence of wild-type profilin (HAARER *et al.* 1993). One possible explanation for the ability of these mutant profilins to provide apparently wild-type levels of profilin function *in vivo* is that they may be overexpressed relative to wild-type profilin, despite being expressed from centromere-based plasmids. To examine this possibility and to provide strains for subsequent synthetic lethal screens (below), we replaced *PFY1* with a mutated gene that encodes a profilin that is partially defective for both actin and PIP_2 binding. This profilin contains an arginine to glutamate change at amino acid position 72; we refer to this mutant profilin allele as *pfy1-111*, as it directs the synthesis of mutant profilin #111 that was previously described by HAARER *et al.* (1993). Strains containing a single copy of the *pfy1-111* allele display some of the mutant phenotypes associated with the total absence of profilin. However, the *pfy1-111* phenotypes are generally less severe. The growth rate of *pfy1-111* cells is slower than that of comparable *PFY1* cells at 22° (Figure 1), although doubling times are only increased ~50–75%, rather than the ~300% increase observed for cells that totally lack profilin (HAARER *et al.* 1990). *pfy1-111* cells also exhibit heterogeneous increases in size, occasionally become multinucleate (10–20% of cells), and display varying degrees of chitin delocalization (Figure 2C; *cf.* the wild-type cells in 2A). Finally, >50% of such cells also accumulate aberrant actin bars (Figure 2D; *cf.* the wild-type cells in 2B), similar to those observed in *pfy1*Δ cells (HAARER *et al.* 1990). As with *pfy1*Δ cells, these actin bars are situated adjacent to the nucleus (unpublished observations).

pfy1-111 cells also display a moderate temperature sensitivity at 37° (Figure 1). The arrest morphology is quite heterogeneous, although *pfy1-111* cells do not show as dramatic an increase in size as do *pfy1*Δ cells (HAARER *et al.* 1990). Interestingly, *pfy1-111* cells incubated at 37° often display actin localization that is coincident with the DAPI-stained nucleus (Figure 2, E and F). The frequency of this occurrence ranges from <1% at permissive temperature to 18% after 4 hr at 37°.

Identification of mutations that enhance the phenotype of *pfy1-111* cells: We are interested in identifying proteins that interact with profilin to help it perform its normal functions, *e.g.*, in responding to cellular signals and in regulating the actin cytoskeleton. To this end, we sought mutations that exacerbate the *pfy1-111* phenotype (so-called "synthetic lethal" mutations; BENDER and PRINGLE 1991; HOLTZMAN *et al.* 1993). Using the adenine color-sectoring assay described by BENDER and PRINGLE (1991), we have identified mutations that are synthetically lethal with the *pfy1-111* point mutation. To perform the assay, we used strain BHY14*, which is BHY14 (*ade2, ade3, his3, ura3, pfy1-111*) bearing the high-copy-number plasmid pTSV-PFY (2μ, *HIS3, ADE3, PFY1*). BHY14* forms red colonies due to the *ade2* mutation, with white sectors that result from loss of plasmid pTSV-PFY, yielding an *ade2 ade3* genotype. Acquisition of a *pfy1-111*-enhancing, or synthetic-lethal, mutation by BHY14* will result in a requirement for the plasmid-borne *PFY1* gene; the resulting colonies will be entirely red.

From screening a relatively small number of UV-mutagenized colonies (~5000), we identified five strains [referred to as NS(14)1, 4, 8, 14, and 24] that consistently showed either no sectoring (Sect$^-$) or greatly reduced sectoring and that survived the following tests. Each of these strains was shown to reacquire the sectoring (Sect$^+$) phenotype upon transformation with a second *PFY1*-containing plasmid (2μ, *URA3, PFY1*), demonstrating (1) a need for *PFY1* rather than for some other gene contained on the primary plasmid, and (2) that the original plasmid had not integrated into one of the host strain's chromosomes, which would also result in a Sect$^-$ phenotype. Each strain was also crossed

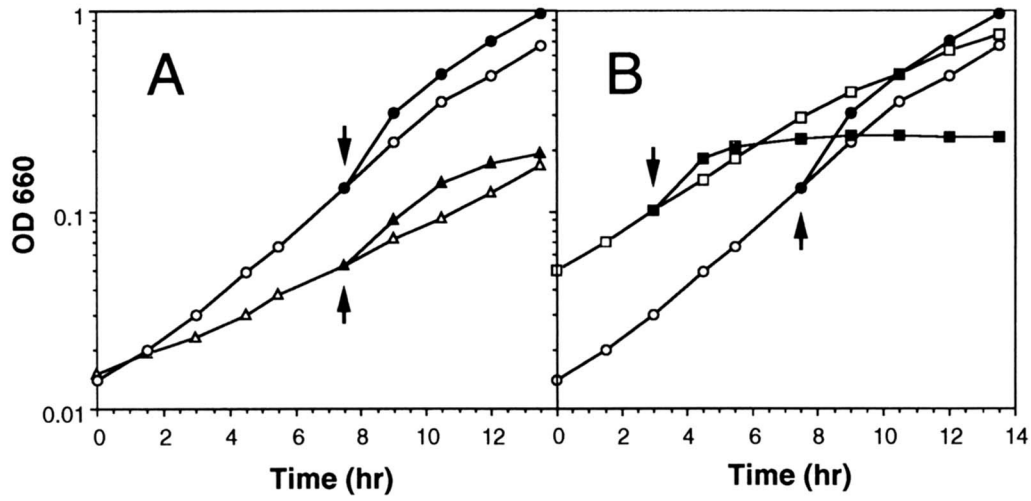

FIGURE 1.—Growth curves and temperature shifts for *pfy1-111* and *psl1-1* (*sec3-101*) strains. Cells were grown in SC medium to mid-log phase at 22°. At the indicated times (arrows), a portion of each culture was then shifted to 37° (closed symbols) or maintained at 22° (open symbols). (A) Comparison of *pfy1-111* homozygous diploid (BHY48; triangles) to wild-type control cells [(DC5xY388)2D+13A; circles]. (B) Comparison of *psl1-1* homozygous diploid (BHY47; squares) to the same wild-type control as shown in A.

to BHY46 (*ade2, ade3, pfy1-111*); for tetrads in which each spore maintained plasmid pTSV-PFY, 2:2 segregation of the Sect$^-$ phenotype indicated a single synthetic lethal mutation. Further, these strains were crossed to a *PFY1* strain [(DC5xY388)10A] to show that the Sect$^-$ phenotype was not due to a second mutation in the profilin gene or to a requirement for multiple copies of the profilin gene (a multicopy suppressee phenotype; BENDER and PRINGLE 1991), either of which would result in 2:2 segregation of the Sect$^-$ phenotype. Instead, we observed the expected segregation patterns of 4:0, 3:1, and 2:2 (Sect$^+$:Sect$^-$) in roughly a 1:4:1 ratio, in each case indicating a synthetic lethal mutation that is unlinked to the *PFY1* locus.

Crosses to BHY46 (above) also indicated that each of the mutations is recessive. Pairwise genetic crosses between strains showed that the five synthetic lethal mutations fall into separate complementation and linkage groups. Furthermore, no pair of mutations was synthetically lethal with each other in the *pfy1-111* back-

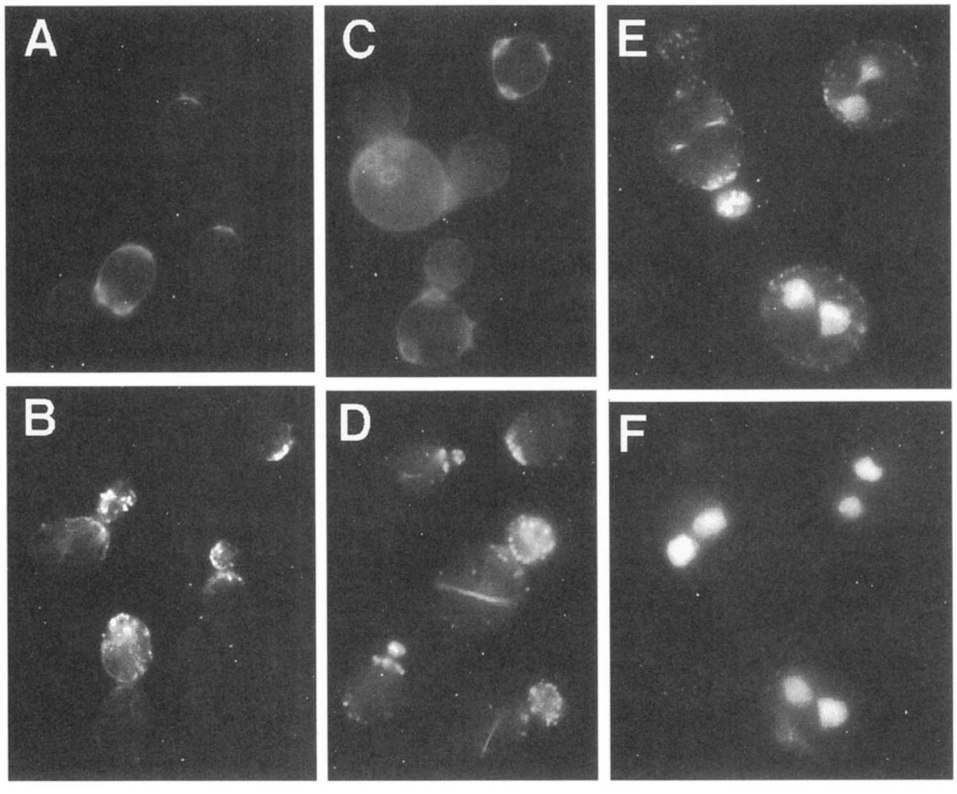

FIGURE 2.—Characterization of *pfy1-111* strains. Calcofluor (A, C), anti-actin (B, D, E), and DAPI staining (F) of wild-type [strain (DC5xY388)2D+13A; A, B] and *pfy1-111* (strain BHY48, C–F) cells grown at ~22° (A–D), or after 4 hr at 37° (E, F).

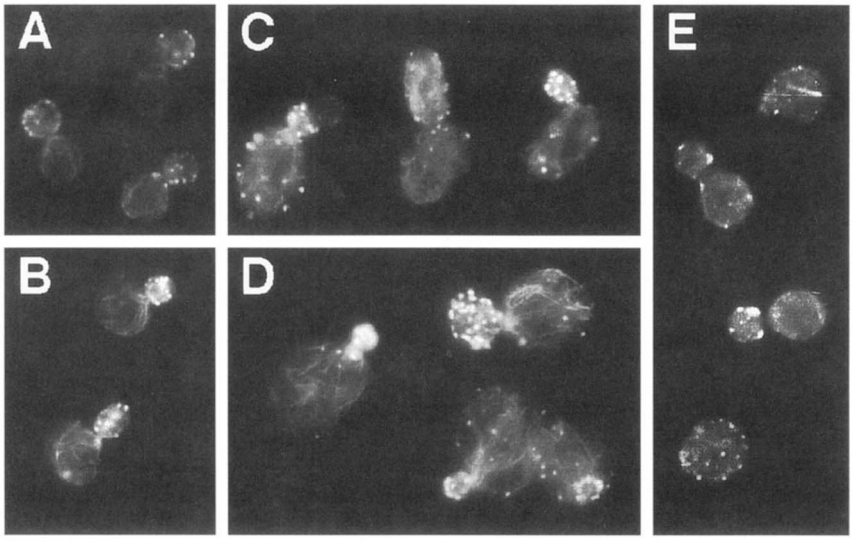

FIGURE 3.—Actin staining of *psl* strains. Representative *psl* haploid strains were stained with anti-actin antibodies after growth at ~22° (A–D) or after 5.5 hr at 37° (E). (A, E) Strain BHY43 (*psl1-1* = *sec3-101*); (B) strain BHY33 (*psl2*); (C) strain BHY35 (*psl3*); (D) combination of cells from strains BHY37 and BHY38 (*psl4*).

ground (in the presence of plasmid pTSV-PFY), nor did any of these mutations suppress the synthetic lethality between any of the other mutations and *pfy1-111*. We will refer to the mutated genes in these strains as *psl1* to *psl5* (profilin synthetic lethal), respectively. While *psl5* strains met these criteria for synthetic lethality, the Sect$^-$ phenotype proved to be somewhat leaky and may be reverting at relatively high frequency. Therefore, we chose not to characterize these strains further.

Phenotypic analysis of *psl* mutants: Upon confirmation that the profilin synthetic lethal interaction was due to a single mutation and that this mutation was not at the profilin locus, we sought to further characterize the phenotypic effects of these mutations. Cells containing the *psl1* mutation are slightly rounder than normal, but display little abnormality in phenotype beyond this (see Figure 3A). The general morphology of *psl2*-containing strains is indistinguishable from wild-type control cells; *psl3* and *psl5* cells are slightly elongated. *psl4* cells look essentially wild type in shape, but tend to be slightly larger than corresponding wild-type haploid or diploid strains. The phenotypic effects of these mutations were essentially the same either in *PFY1* strains, or in *pfy1-111* strains carrying plasmid-borne *PFY1*.

Despite the presence of plasmid-borne *PFY1*, which complements the *pfy1-111* temperature sensitivity, we found that *psl1*, *psl3*, and *psl4* strains are temperature-sensitive for growth. In crosses of the original *psl1*, *psl3*, and *psl4* Sect$^-$ strains to BHY46, temperature sensitivity cosegregated with the Sect$^-$ phenotype (12 tetrads were dissected for each cross, with 44, 42, and 45 viable segregants for the *psl1*, *psl3*, and *psl4* crosses, respectively). Indeed, the *psl1*, *psl3*, or *psl4* mutations in a *PFY1* background result in temperature-sensitive growth. *psl1* strains arrest at 32°, while *psl3* and *psl4* strains arrest at 37–38°. *psl1* strains displayed the tightest arrest; after shifting from 22° to 37°, cells carrying the *psl1-1* mutation underwent approximately one doubling (Figure 1B), with cells displaying a heterogeneous arrest with respect to cell-cycle position, as judged by bud size (see Figure 3E). Strains carrying *psl3* or *psl4* mutations also fail to show uniform arrest at restrictive temperature (data not shown).

To see if any of the *psl* mutations directly affect actin localization, we stained *psl* strains with anti-actin antibodies. Actin localization varies in the *psl* strains (Figure 3), but there do not appear to be gross abnormalities when cells are grown at room (permissive) temperature. In general, *psl2* and *psl4* strains (Figure 3, B and D, respectively) have normal actin staining patterns (HAARER *et al.* 1990; WELCH *et al.* 1994). Actin cables were somewhat fainter in *psl1* and *psl3* strains (Figure 3, A and C, respectively), but polarization of the actin cytoskeleton was similar to that of wild-type control strains. Homozygous diploid strains had essentially the same actin staining patterns as haploid *psl* strains (data not shown). Upon shift to 37°, wild-type and *psl* strains displayed the expected depolarization of the actin cytoskeleton (LEW and REED 1993; LILLIE and BROWN 1994). After 2 hr, the actin cytoskeleton of *psl2* strains recovered to an extent comparable to wild-type controls, although even the control strains displayed reduced staining of actin cables and an increased frequency of random cortical actin spots (data not shown). At 2 and 4 hr postshift, *psl3* and *psl4* strains showed some recovery of cortical spot polarization, but actin cables were either very faint (*psl4*) or not visible (*psl3*) by antibody labeling (not shown). There was essentially no recovery of the actin staining pattern in *psl1* strains (Figure 3E). Instead, a significant number of such cells contained actin bars.

***psl1*, *psl3*, and *psl4* mutants are defective in α-factor production:** Using a halo assay, we had previously shown that *pfy1*Δ haploid cells are defective in α-factor production or secretion. We thus sought to determine if any of the *psl* mutations had a similar effect on α-factor production or secretion. *psl1-1 MAT*α and *pfy1-*

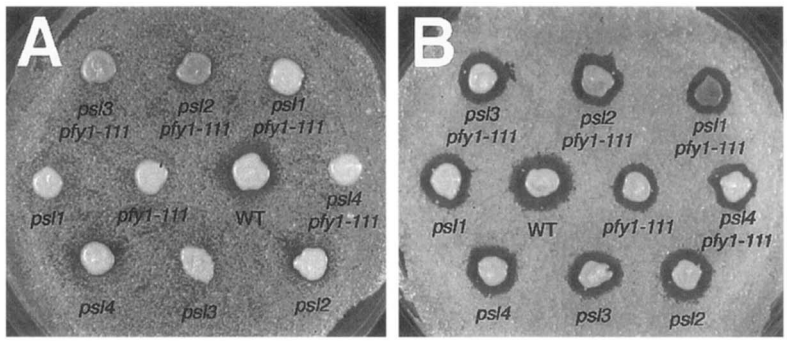

FIGURE 4.—Halo assays for α- and **a**-factor production by *psl* and *pfy1-111* strains. Representative strains were spotted on lawns of XMB**a** (A) or αsst2 (B). Relevant genotypes are indicated; the mutant strains were BHY17, 18, 21–24, 26, 27, 33–38, and 43–48; the wild-type (WT) strains tested were (DC5xY388)2D and (DC5xY388)13A.

*111 MAT*α strains elicit reduced halo formation on lawns of *MAT***a** *bar1* cells (strain XMB4**a**), while *psl2 MAT*α strains produce relatively normal halos (Figure 4A). As *bar1* strains are supersensitive to arrest by α-factor, the size of the halo (region of growth inhibition) is proportional to the amount of α-factor being secreted by the *MAT*α strain. No visible halos are detected when *psl3 MAT*α strains are plated on XMB4**a;** the response of *psl4 MAT*α strains varies from no halo to small halo depending on strain background (Figure 4A). When examined microscopically, shmooing of XMB4**a** cells immediately adjacent to the spotted *psl3* or *psl4* strains could be detected, suggesting that some functional α-factor is being secreted. Formation of halos by *psl MAT***a** strains was normal on lawns of *MAT*α *sst2* cells (an **a**-factor supersensitive strain), indicating normal production of **a**-factor by these strains (Figure 4B). Thus, *psl1, psl3, psl4* and *pfy1-111* strains are at least partially defective in the release of α-factor, indicating potential defects in the ER-directed secretory pathway.

Osmotic sensitivity of *psl3* and *pfy1-111* strains: Mutations in the yeast actin gene (*ACT1*) can cause strains to become super-sensitive to increased osmolarity of the growth media (NOVICK and BOTSTEIN 1985; CHOWDHURY *et al.* 1992). Thus, one might expect mutations that affect the actin cytoskeleton to confer a similar osmosensitive phenotype. To examine this possibility, we tested various *pfy1-111* and *psl* strains on YEPD plates containing 1.2 M KCl or 1.8 M sorbitol (CHOWDHURY *et al.* 1992). Not surprisingly, *pfy1-111* mutants were moderately sensitive to the high osmolarity medium when compared to other strains tested. Of the *psl* mutant strains, only *psl3*-containing haploid [NS(14)8, BHY35, and BHY36] and diploid (BHY58) strains are osmosensitive. These strains exhibited reduced growth rate relative to wild type, but were not killed on high osmolarity medium.

The *psl* mutations are not in *ACT1* or *CAP/SRV2*: The demonstrated *in vitro* interactions between profilin and actin suggested that one of the *psl* mutations could likely be in the yeast actin gene. Because transformation of representative strains carrying each of the *psl1* to *psl5* mutations with an *ACT1*-containing centromere plasmid (provided by K. WERTMAN and D. DRUBIN) did not promote sectoring, none of the *PSL* genes is *ACT1*.

Since mutations in the *CAP/SRV2* gene can be suppressed by multiple copies of *PFY1* (VOJTEK *et al.* 1991), we also examined the ability of a plasmid expressing *CAP/SRV2* (pADH-CAP; GERST *et al.* 1991) to promote sectoring of *psl* strains. This plasmid failed to promote sectoring of the *psl* strains, indicating that the *psl1* to *psl5* mutations are not in *CAP/SRV2*.

Cloning of *PSL1*: To clone the wild-type *PSL1* gene, we transformed the Sect$^-$, Ts$^-$ strain NS(14)1 (*ade2, ade3, his3, ura3, psl1, pfy1-111,* plus plasmid pTSV-PFY) with a yeast genomic library made in the low-copy-number vector YCp50, and screened for the appearance of Ura$^+$, Sect$^+$ transformants at 22°. Two sectoring colonies were identified and were restreaked on medium lacking uracil to confirm the Sect$^+$ phenotype. Further testing at 37° showed that the temperature sensitivity of NS(14)1 was complemented in only one of the transformants. The library plasmid from the Ts$^-$ transformant was later found to contain *PFY1*.

A plasmid from the Ts$^+$ transformant was recovered in *E. coli* and its ability to transform the *psl1* strain to Ts$^+$ and Sect$^+$ was confirmed. That this plasmid contained the authentic *PSL1* gene was shown as follows. (1) A noncomplementing fragment from the plasmid insert was cloned into a yeast integrative plasmid (YIp5), which was then linearized within the insert and used to transform strain NS(14)1 via homology-mediated recombination. Four Ura$^+$ transformants were shown to be completely stable for the Ura$^+$ phenotype, indicating that the plasmid had integrated into the yeast genome. These transformants were mated with strain BHY46 (*pfy1-111, ura3, PSL1*) followed by sporulation and tetrad analysis. In each case, the Ura$^+$ phenotype cosegregated with the nonsectoring phenotype and temperature sensitivity caused by *psl1*. (2) Marker rescue experiments (see MATERIALS AND METHODS) were also used to show that the cloned DNA corresponds to the *PSL1* gene (Figure 5A). This technique localized the probable *psl1-1* mutation to a 750-bp region flanked by *Sst*I and *Nco*I sites.

***PSL1* is the same as *SEC3*:** Genetic mapping data (see MATERIALS AND METHODS) indicated that the *PSL1* gene is tightly linked to the centromere of chromosome *V*, in the vicinity of the previously mapped but uncloned secretory pathway gene *SEC3*. The map position, simi-

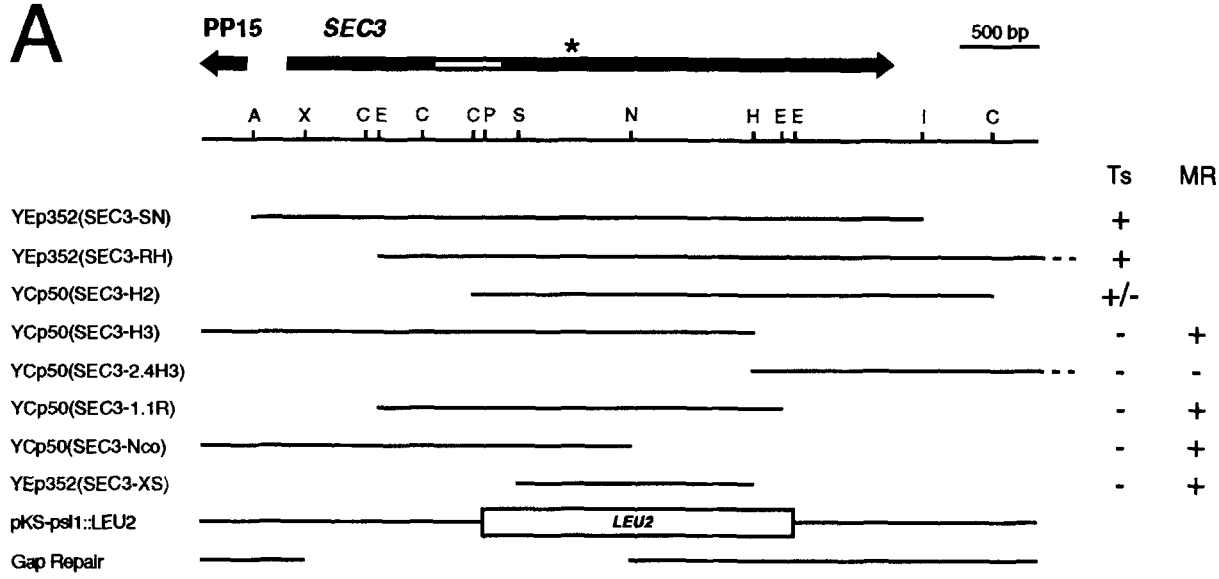

FIGURE 5.—Restriction map and nucleotide sequence of the *SEC3* (*PSL1*) locus. (A) Restriction map and subcloning of the *SEC3* locus. The heavy arrows denote the *SEC3* and partial upstream (PP15) open reading frame; the designation PP15 refers to the similarity between this open reading frame and mammalian placental protein 15 (GRUNDMANN *et al.* 1988), which is likely to be a factor important for the transport of proteins into the nucleus (MOORE and BLOBEL 1994). The open box in the *SEC3* arrow represents the predicted coiled-coil region; the asterisk corresponds to the nonsense codon of *sec3-101* (*psl1-1*). The pKS-psl1::LEU2 line shows the region deleted in the *sec3*Δ*::LEU2* allele (the *LEU2* region is not drawn to scale); the missing region of the Gap Repair line indicates the *sec3-101*-containing region that was cloned from strain BHY47. The Ts column indicates the ability of subclones to complement the temperature sensitivity of *sec3-101* strains; MR indicates the ability (+) or inability (−) of noncomplementing fragments to rescue the *sec3-101* mutation. Restriction sites are as follows: A, *Sca*I; C, *Hind*II; E, *Eco*RI; H, *Hind*III; I, *Nsi*I; N, *Nco*I; P, *Pvu*II; S, *Sst*I; X, *Xba*I. (B) Nucleotide sequence of *SEC3* and flanking DNA. Protein translations are given for Sec3p and the upstream open reading frame. Nucleotide positions are numbered from the beginning of the sequence and are presented on the right; amino acid positions for *SEC3* and the upstream open reading frame are presented on the left. The region of *SEC3* predicted to form coiled-coil structure (*cf.* Figure 6) is bracketed and shown in italics; the *Pvu*II site used in creating the *sec*Δ*::LEU2* mutation is underlined; the two amino acids known to be affected in the *sec3-101* allele are indicated by larger bold letters. The Genebank accession number for the *SEC3/PSL1* nucleotide sequence is L22204.

larity of the *psl1* arrest phenotype to that of *sec3* mutants, and other genetic data (A. CORBETT and P. SILVER, unpublished data) led us to suspect that the *PSL1* gene was equivalent to *SEC3*. This is in fact the case, as the *PSL1* clone was able to complement the temperature sensitivity of *sec3* strains, and *psl1-1* showed tight linkage to *sec3* (no recombinants in 30 tetrads). In addition, P. NOVICK and F. FINGER (personal communication) have cloned the same gene by complementation of *sec3* strains. Therefore, we will hereafter refer to *PSL1* as *SEC3* and the *psl1-1* allele as *sec3-101*.

Sequence analysis of *SEC3/PSL1*: Sequence analysis of the *sec3*-complementing subclone revealed a large open reading frame of 1336 codons (Figure 5B), potentially encoding a polypeptide of molecular weight 154,683 and predicted isoelectric point of 5.18. Subcloning experiments (Figure 5A) showed that a 4.4-kb *Sca*I-*Nsi*I fragment containing this open reading frame and ~230 and ~190 bp of upstream and downstream noncoding sequence, respectively, is able to fully complement the temperature sensitivity of *sec3-101* strains and the Sec$^-$ phenotype of *sec3-101 pfy1-111* strains. In addition, this region contains the ~750 bp *Sst*I-*Nco*I DNA fragment shown to rescue the *sec3-101* mutation. Analysis of predicted secondary structure revealed a region of the putative Sec3 polypeptide that is quite hydrophilic and strong in α-helical structure. Further analysis of this region using the program of LUPAS *et al.* (1991) has indicated a strong probability that the region from codon ~320 to ~465 forms coiled-coil secondary structure (Figure 6). Such a structure may be involved in protein dimerization (LUPAS *et al.* 1991).

Interestingly, a subclone that truncates the 5′ end of the putative coding region by as many as 200 codons [Figure 5A; YEp352(SEC3-RH)] retains the ability to complement the temperature sensitivity of *sec3-101* strains. Indeed, even truncation to codon 408 [YCp50(-SEC3-H2)] retains partial complementing ability. Expression of the latter clone from a high-copy-number 2μ vector resulted in better complementation of temperature sensitivity, although the ability to complement was dependent upon the orientation of the cloned fragment within the vector, suggesting that gene expression was directed from a fortuitous promoter element located within the vector sequences. We have not eliminated the possibility that the Sec3p coding region initiates at a downstream ATG; the closest in-frame ATG sites are at codons 192 and 308. Indeed, complementation by truncated clones may rely on one of these downstream sites for translation initiation.

B

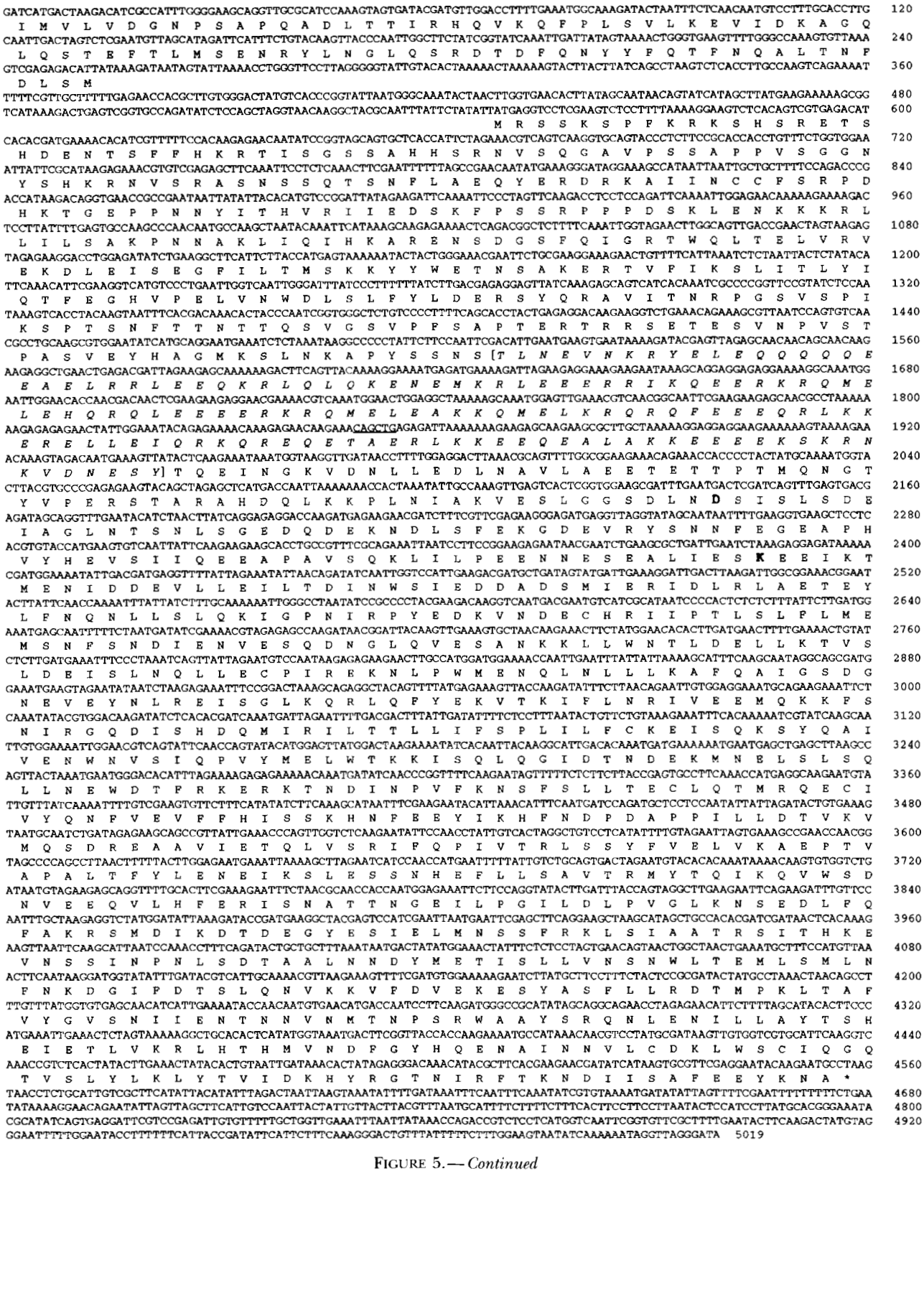

FIGURE 5.—*Continued*

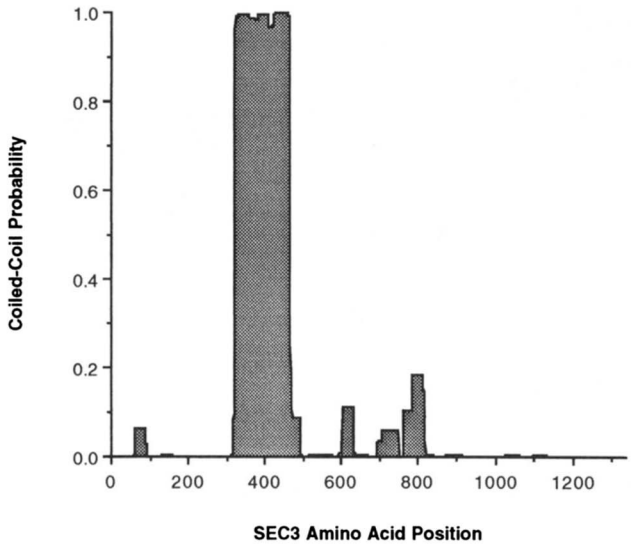

FIGURE 6.—Coiled-coil analysis of Sec3p. The algorithm of LUPAS *et al.* (1991) was used to predict regions of potential coiled-coil secondary structure in the putative Sec3 protein. Coiled-coil probability is plotted as a function of amino-acid position.

Partial deletion of the *SEC3* coding region and analysis of the *sec3-101* mutant: A portion of the *SEC3* gene was replaced with the *LEU2* gene (see MATERIALS AND METHODS), effectively truncating the protein at codon 434 (Figure 5). Tetrad analysis of a diploid heterozygous for this partial deletion suggested that *SEC3* was essential for growth on YEPD rich medium at 22° (Figure 7). However, incubation of spores on supplemented SD medium resulted in growth of all four segregants, with two segregants per tetrad showing a slightly reduced growth rate (Figure 7). Upon continued incubation (10–14 days), colonies eventually grew from the third and fourth YEPD-grown spores (not shown). This rich-medium sensitivity is also exhibited by strains carrying the *sec3-101* allele and is examined further below.

The *Sst*I-*Nco*I segment indicated by marker rescue experiments to contain the *sec3-101* lesion (see Figure 5A) was recovered from a *sec3-101* strain by plasmid gap repair (see MATERIALS AND METHODS). The sequence of this 750-bp region contained five nucleotide differences as compared to the DNA sequence determined from the *SEC3* library isolate. Three of these nucleotide changes are silent (T to C in codon 686, A to G in codon 715, and T to C in codon 736), a fourth G to T difference changes amino acid 531 from aspartate to tyrosine, and the fifth difference creates a nonsense TAA codon at position 613 (normally lysine). Presumably, the three silent changes and perhaps the missense mutation simply represent polymorphisms between the *SEC3* gene of strain BHY47 (the source of *sec3-101*) and the strain from which the YCp50 library was constructed. Assuming the nonsense codon at position 613 is the primary defect of the *sec3-101* allele, it is interesting to note that the C-terminal 720 amino acids are largely dispensable for vegetative growth on synthetic defined media at 22°. Moreover, the partial deletion of *SEC3* described above only removes an additional 179 amino acids, and both situations leave the majority of the coiled-coil region intact. Thus, it is perhaps not surprising that the *sec3-101* and *sec3*Δ*::LEU2* alleles behave similarly.

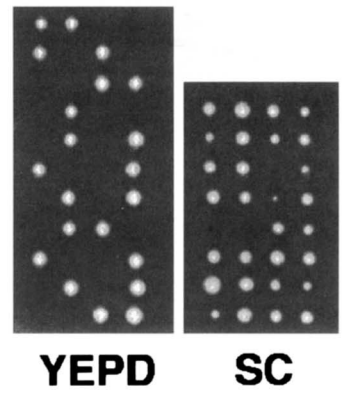

FIGURE 7.—Effects of *sec3* partial deletion on cell growth. A *sec3* deletion heterozygote (see MATERIALS AND METHODS) was sporulated and tetrads were dissected on YEPD or SC medium and incubated at ~22° for 4 (YEPD) or 8 (SC) days.

Rich medium sensitivity of *sec3* strains: During the course of crossing our *sec3-101* strains, it became apparent that they grew more slowly on YEPD than on synthetic medium, regardless of whether the SD was provided with the 16 nutritional supplements as described by SHERMAN *et al.* (1986), or just those required to support growth of the particular yeast strain. This is true for the original *psl1/sec3* strain NS(14)1, *sec3-101* strains in *PFY1* backgrounds, and strains that are lacking a substantial portion of the *SEC3* gene (see above). While this rich-medium sensitivity is not absolute, growth is decidedly retarded on YEPD. As with temperature sensitivity, amino-terminally truncated *SEC3* clones can provide full to partial complementation, depending on the degree of truncation. Attempts to determine what component in rich medium retards growth have thus far met with little success. Strains partially defective in *CAP/SRV2* function are somewhat sensitive to valine concentration (VOJTEK *et al.* 1991). However, SD plates containing excess valine supported normal growth of *sec3-101* strains. By adding concentrated stocks of yeast extract or peptone (YEPD components) to SD plates, we determined that the peptone was providing the putative inhibitory factor. Addition of a 10-fold excess of arginine, cysteine, glycine, tyrosine, or glutamate (amino acids that are especially enriched in peptone) to synthetic medium did not significantly retard growth of the *sec3* strains. Given profilin's potential involvement in PIP_2 metabolism, we also tested *sec3* strains for sensitivity to excess inositol, but found that up to 10 mM inositol had no significant effect on the growth of these strains. Finally, we also determined that pH differences do not account for the rich-medium sensitivity. Growth

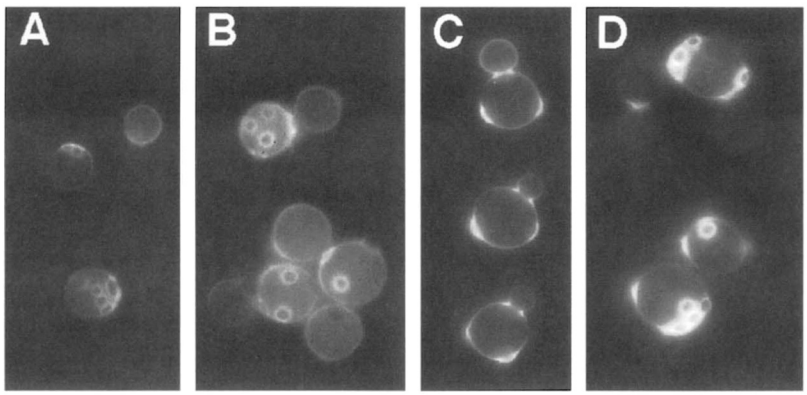

FIGURE 8.—Bud scar patterns of *sec3* haploid and diploid cells. *sec3* haploid and homozygous diploid cells with or without *SEC3*-containing plasmids were stained with Calcofluor to determine budding polarity. (A) Strain BHY43 (*sec3-101*); (B) strain BHY47 (*sec3-101/sec3-101*); (C) strain BHY47 containing control plasmid YEp352; (D) strain BHY47 containing YCp50-SEC3.

of yeast on our SD plates (normally pH 5) acidifies the media to pH 3.0–3.5, while growth on YEPD only results in a change from pH 6.5–7.0 to pH 6. Buffering of SD plates to pH 6 enhanced, rather than inhibited, the growth of our *sec3* strains.

***SEC3* mutant strains are defective in diploid-specific bud-site selection:** In budding yeast, chitin is normally laid down in the cell wall in discrete rings through which the growing bud emerges. In haploid cells, these rings are concentrated at a single pole of the ellipsoidal cell (axial budding), while diploid cells are able to bud from either end of the cell (bipolar budding). Failure to properly target secretion can lead to more generalized deposition of chitin throughout the cell wall. Defects in actin, profilin, or other actin-regulatory proteins can often lead to random or near random deposition of chitin, suggesting that actin may play an important role in establishing or maintaining targeted secretion. The ability of *sec3-101* haploid cells to properly organize chitin rings was determined by staining with Calcofluor (Figure 8). While there may be a slight increase in the mislocalization of cell wall chitin, these cells generally form normal chitin rings in a proper axial pattern. Staining of homozygous *sec3-101* diploids demonstrated that these cells are also able to organize discrete chitin rings. However, rather than budding in a bipolar fashion, these cells largely exhibit random patterns of chitin rings in the mother-cell wall (Figure 8; Table 2). Thus, homozygous *sec3* diploid cells, while not grossly defective in localized secretion at permissive temperature, are unable to maintain the normal cellular polarity necessary for bipolar budding. This diploid-specific budding defect can be partially cured by plasmid-borne full-length or amino-terminally truncated *SEC3*, but not by multiple copies of profilin (Table 2). Finally, we have also shown that haploid segregants derived from *sec3* mutant diploid cells regain normal (axial) budding polarity (Table 2), demonstrating that secondary budding mutations are not acquired during the formation or subsequent growth of diploid *sec3/sec3* strains. These observations, coupled with similar effects in other strains (BAUER *et al.* 1993; SIVADON *et al.* 1995; BÉNÉDETTI *et al.* 1994), lend support to arguments for inherent differences between axial and bipolar budding mechanisms (see DISCUSSION).

To explore the possibility that the observed bud-site selection defects are simply due to the generalized disruption of normal secretory processes, we examined the budding patterns of other secretory mutants. As shown in Table 3, diploids homozygous for mutations in early (*sec18*), middle (*sec7*), or late (*sec1, sec2,* or *sec6*) secretory pathway genes displayed normal bipolar budding. Thus, the bipolar budding defect is not a general effect of perturbing the secretory pathway, and may indicate a more specialized role for the *SEC3* gene product. Interestingly, *pfy1-111* strains exhibit a similar diploid-specific budding defect (Table 2). This is in contrast to *pfy1*Δ cells, which bud randomly as haploids (HAARER *et al.* 1990).

Additional synthetic interactions between mutations in *PFY1* and other genes: Given the observed synthetic lethality between *pfy1-111* and *sec3-101,* we sought to determine if there were synthetic interactions between *pfy1-111* and mutations in other late-acting *SEC* genes. Combinations of *pfy1-111* with *sec2-41, sec4-8, sec8-9,* or *sec9-1* were either synthetically lethal or generated very slow growing cells, while combinations with *sec1-1, 5-25, 6-4, 7-1, 10-2, 15-1, 18-1* resulted in little or no reduction in growth rate (Table 4). We further found that cells carrying the *pfy1-111* mutation and a deletion of the endocytosis gene *END3* display a severe synthetic phenotype (Table 4).

As many late-acting *SEC* genes also show synthetic lethal interactions with mutations in *MYO2* and *SMY1* (myosin- and kinesin-related genes, respectively, whose products are apparently involved in late stages of secretion; LILLIE and BROWN 1992, 1994; GOVINDAN *et al.* 1995), we examined such combinations with *pfy1-111* as well. While there might be a slight reduction in growth rate when the *pfy1-111* mutation is combined with *myo2-66* or *smy1* deletion alleles, the effects are minimal (Table 4).

We also examined potential synthetic interactions between *pfy1-111* and mutations in other genes affecting actin function. As indicated in Table 4, *pfy1-111* is synthetically lethal with *act1-2* and is quite sick in combina-

TABLE 2

Bud site selection in *sec3* and *pfy1-111* strains

Strain	Relevant genotype[a]	+ plasmid	Budding pattern (%)[b]		
			Unipolar	Bipolar	Random
BHY43	*MAT***a** *sec3-101*	None	91[c]	5	4
BHY44	*MATα sec3-101*	None	90[c]	2	8
BHY47	*MAT***a**/*MATα sec3-101/sec3-101*	None	10	21	69
(DC5xY388)2D	*MATα*	None	97	2	1
(DC5xY388)13A	*MAT***a**	None	99	0	1
(DC5xY388)2D+13A	*MAT***a**/*MATα*	None	38	60	2
BHY45	*MATα pfy1-111*	None	98	1	1
BHY46	*MAT***a** *pfy1-111*	None	99	1	0
BHY48	*MAT***a**/*MATα pfy1-111/pfy1-111*	None	8	11	81
BHY47-1A	*MAT***a**/*MATα sec3-101*	None	97[c]	0	3
BHY47-1B	*MAT***a**/*MATα sec3-101*	None	90[c]	1	9
BHY47-1C	*MAT***a**/*MATα sec3-101*	None	93[c]	2	5
BHY47-1D	*MAT***a**/*MATα sec3-101*	None	96[c]	0	4
BHY47	*MAT***a**/*MATα sec3-101/sec3-101*	YCp50	4	23	73
BHY47	*MAT***a**/*MATα sec3-101/sec3-101*	YCp50(SEC3)	33	49	18
BHY47	*MAT***a**/*MATα sec3-101/sec3-101*	YEp352(SEC3-RH)	23[c]	57	20
BHY47	*MAT***a**/*MATα sec3-101/sec3-101*	YEp420(PFY1)	14[c]	18	68
BHY51	*MAT***a** *sec3Δ::LEU2*	None	93	1	6
BHY52	*MATα sec3Δ::LEU2*	None	94	1	5
BHY63	*MAT***a**/*MATα sec3Δ::LEU2/sec3Δ::LEU2*	None	9	10	81

[a] The *sec3-101* allele is equivalent to *psl1-1*.
[b] Unless otherwise indicated, $N = 200$; see MATERIALS AND METHODS for an explanation of budding patterns.
[c] $N = 100$.

tion with *act1-3*. *pfy1-111* is also synthetically lethal with a deletion of *SLA2*, which itself was identified via genetic interactions with the gene encoding Abp1p, an actin-binding protein (HOLTZMAN *et al.* 1993). [Interestingly, *SLA2* was also identified as *END4* due to its role in endocytosis (BÉNÉDETTI *et al.* 1994), and as *MOP2* due its requirement for the maintenance of normal levels of plasma membrane H^+-ATPase at the cell surface (NA *et al.* 1995).] Finally, there does not appear to be any exacerbation of phenotypes when *pfy1-111* is combined with a deletion of the actin-capping protein gene, *CAP2*.

DISCUSSION

We have replaced the wild-type yeast profilin gene with a mutated form that changes codon 72 from arginine to glutamate. While the profilin produced from this gene is severely affected in its ability to interact with actin and PIP_2 *in vitro* (HAARER *et al.* 1993), it clearly retains a substantial fraction of its normal *in vivo* function. This would suggest either that the actin- and PIP_2-binding activities of profilin are normally present in great excess, or that some other less affected property of profilin, perhaps polyproline binding, is more important for its *in vivo* activity. A third possibility is that this mutant profilin is stabilized *in vivo* through its association with other factors and that the measured *in vitro* properties do not accurately reflect the *in vivo* activity of this protein.

Significance of profilin synthetic lethal mutants to profilin and actin function: Synthetic lethality screens

TABLE 3

Bud site selection in diploid strains defective in secretion

Relevant genotype	Portion of secretory pathway affected[a]	Budding pattern (%)[b]		
		Unipolar	Bipolar	Random
sec1-1/sec1-1	Late	28	70	2
sec2-70/sec2-70	Late	29	70	1
sec6-4/sec6-4	Late	26	72	2
sec7-1/sec7-1	Middle	27	70	3
sec18-1/sec18-1	Early	36	64	0
SEC+/SEC+	None	42	57	1

[a] Early, endoplasmic reticulum to Golgi; middle, Golgi to secretory vesicle and Golgi to vacuole; late, secretory vesicle to plasma membrane.
[b] $N = 200$; see MATERIALS AND METHODS for an explanation of budding patterns.

TABLE 4

Synthetic interactions with *pfy1-111*

Synthetically lethal with *pfy1-111*	Synthetically sick with *pfy1-111*	Little/no synthetic interaction with *pfy1-111*
sec2-41	*sec8-9*	*sec1-1*
sec4-8	*sec9-1*	*sec5-25*
sla2Δ/end4Δ	*end3Δ*	*sec6-4*
act1-2	*act1-3*	*sec7-1*
		sec10-2
		sec15-1
		sec18-1
		myo2-66
		smy1Δ
		cap2Δ

have generally been performed using null mutant alleles in cases of nonessential or redundant genes (BENDER and PRINGLE 1991; HOLTZMAN *et al.* 1993). The use of silent or attenuated mutant alleles permits the use of this screen with essential (or nearly essential) genes. Moreover, knowledge of the *in vitro* effects of such mutations may allow one to target specific classes of synthetic lethal mutations. In this study, we have used the *pfy1-111* allele in screens for synthetic lethal mutations. The *in vitro* properties of the profilin encoded by this mutant gene suggested that one might identify mutations that relate to profilin's actin- or PIP_2-binding properties (HAARER *et al.* 1993). In a relatively small screen, we have identified four tight synthetic lethal mutations, *psl1–psl4,* and a fifth, somewhat leaky, mutation (*psl5*).

Several lines of evidence suggest that these *psl* genes are relevant to profilin's normal functions, particularly to its involvement with the actin cytoskeleton. First, three of the mutations (*sec3/psl1, psl3,* and *psl4*) result in a reduction of α-factor secretion or production, as does the *pfy1-111* mutation. The fact that **a**-factor production and secretion are apparently unaffected suggests that the defect is in the ER-mediated secretory pathway, since α-factor traverses this pathway and **a**-factor is exported directly from the cytoplasm. Prior evidence has shown that both actin and profilin mutants are defective in the polarized secretion of cell wall components (NOVICK and BOTSTEIN 1985; HAARER *et al.* 1990) and that actin localizes to sites of new cell wall deposition (ADAMS and PRINGLE 1984). Further, actin mutants demonstrate an accumulation of secretory vesicles and a partial inhibition of invertase secretion (NOVICK and BOTSTEIN 1985). Thus, actin, profilin, Sec3p, Psl3p, and Psl4p all appear to be important for localized secretion. The synthetic lethality between the *pfy1-111* mutation and mutations in the genes encoding Sec3p, Psl3p, and Psl4p suggests either that the loss of these proteins affects actin function to cause the apparent secretory defect, or that these proteins directly affect the secretory pathway and that cell death results from a combination of these defects with profilin/actin-related secretory defects. The latter seems likely in the case of *SEC3,* alleles of which were originally identified by virtue of their late secretory defects (NOVICK *et al.* 1980, 1981).

Another indication of related function is the osmotic sensitivity of *pfy1-111* and *psl3* mutant strains. Various mutant alleles of the yeast actin gene have been shown to cause sensitivity to hyperosmotic conditions (NOVICK and BOTSTEIN 1985; CHOWDHURY *et al.* 1992). We have shown similar osmotic sensitivity in strains carrying mutations in *PFY1* or *PSL3.* Interestingly, mutants defective in phosphatidylinositol-specific phospholipase C activity are also sensitive to hyperosmotic conditions (FLICK and THORNER 1993). Whether or not this phenomenon indicates a link to profilin-PIP_2 interactions and control of the actin cytoskeleton remains to be determined.

Finally, we have also observed that *psl1/sec3* mutants grow poorly on rich medium. This is also the case for mutants defective in adenylate cyclase-associated protein, CAP/Srv2p (GERST *et al.* 1991). In addition to its interactions with yeast RAS and adenylate cyclase, CAP/Srv2p, like profilin, is able to bind actin monomers and retard their polymerization *in vitro* (FREEMAN *et al.* 1995). The rich medium sensitivity of *cap/srv2* mutants is suppressed by overexpression of profilin (VOJTEK *et al.* 1991), suggesting that profilin may be functionally substituting for CAP/Srv2p in this situation. Alternatively, CAP/Srv2p may help bring profilin to the site of RAS/adenylate cyclase activation to bring about localized changes in the actin cytoskeleton. In support of this model, we have recently detected a physical interaction between profilin and adenylate cyclase, although we do not yet know if CAP/Srv2p participates in this binding (S. PALMIERI and B. HAARER, unpublished results). Another gene, *SNC1,* was originally identified by its ability to suppress the rich-medium sensitivity of *cap/srv2* strains that also carry the activated $RAS2^{val19}$ mutation (GERST *et al.* 1992). Interestingly, yeast lacking both *SNC1* and *SNC2,* yeast homologues of synaptobrevin/VAMP v-SNARE proteins, are also retarded on rich medium and are defective in late stages of secretion (PROTOPOPOV *et al.* 1993). Thus, Sec3p may be participating in a similar pathway, perhaps as an intermediary between Snc1p/Snc2p and the adenylate cyclase complex.

Another, albeit less appealing, explanation for the rich-medium sensitivity of *sec3* and other mutant strains is that the reduced growth rate on defined media may allow such strains to complete all cell cycle functions in an ordered fashion. In other words, the presence of abundant nutrients may cause these strains to attempt cell division before completion of preceding events. If true, this would indicate that these strains are defective in one or more cell cycle checkpoint controls.

The importance of actin and profilin in secretory processes: For quite some time, there have been impli-

cations for an essential role of the actin cytoskeleton in the process of polarized secretion in yeast (ADAMS and PRINGLE 1984; NOVICK and BOTSTEIN 1985), but there were few, if any, direct links between proteins of the secretory apparatus and those controlling the actin cytoskeleton. Our identification of a genetic relationship between profilin and late acting *SEC* genes serves to strengthen the evidence linking the actin cytoskeleton to the process of polarized secretion in yeast. That the *sec3-101* allele is also synthetically lethal with the phenotypically silent *pfy1-112* and *pfy1-116* alleles (Y. KWEON and B. HAARER, unpublished data) further indicates that profilin and Sec3p are likely to be involved in overlapping functions. Indeed, our results suggest that there is a general interdependence of profilin and actin functions with components of the late secretory pathway. Further, we can extend this relationship to include End3p and Sla2p/End4p, both of which are important for endocytosis and for proper organization of the actin cytoskeleton (HOLTZMAN *et al.* 1993; BÉNÉDETTI *et al.* 1994).

Two other genes, *RVS161/END6* and *RVS167,* have also been shown to be involved in endocytosis and maintenance of the actin cytoskeleton (BAUER *et al.* 1993; MUNN *et al.* 1995; SIVADON *et al.* 1995). The proteins encoded by these genes show strong similarity to amphiphysin, a protein found in synaptic vesicles (SIVADON *et al.* 1995), and Rvs167p interacts with actin in two-hybrid screens (AMBERG *et al.* 1995). Despite these connections between cytoskeletal, secretory, and endocytic functions, the fine points of their associations remain to be determined.

SEC3 and bud-site selection: Another interesting effect of perturbing actin cytoskeleton (*PFY1, SLA2/END4/MOP2*), secretory (*SEC3*), and endocytic (*END3, RVS161/END6,* and *RVS167*) functions is the generation of a diploid-specific defect in bud-site selection (this study; BAUER *et al.* 1993; BÉNÉDETTI *et al.* 1994; SIVADON *et al.* 1995). In wild-type haploid *S. cerevisiae* cells of mating type **a** or α, budding occurs almost exclusively at one end of the cell (the axial budding pattern), while diploid **a**/α cells exhibit budding from either end of the cell (bipolar budding) (see reviews by CHANT and PRINGLE 1991; CHANT 1994). Several genes have been identified whose only apparent function is in the process of bud-site selection, *i.e.,* defects in these genes do not alter bud growth, merely bud position on the mother cell. These genes are *RSR1(BUD1), BUD2,* and *BUD5,* which are required for both axial and bipolar budding, and *BUD3, BUD4,* and *AXL1,* which are required only for maintenance of the axial budding pattern (CHANT and HERSKOWITZ 1991; CHANT 1994; FUJITA *et al.* 1994). Thus, *SEC3* and the *END* and *RVS* genes are distinct from the *BUD/AXL* genes by at least two criteria: (1) defects in these genes cause bud-site selection defects only in diploids, and (2) the mutant phenotypes extend beyond bud-site selection to include temperature-sensitivity, moderate actin cytoskeleton defects, and partial delocalized secretion of cell wall components. Thus far, *PFY1* appears to be unique in that its effects on budding are allele specific; the *pfy1-111* allele causes budding defects similar to those of *sec3* strains (Table 2), while the *pfy1*Δ allele causes random budding even in haploid cells (HAARER *et al.* 1990).

It has been proposed that the axial and bipolar budding patterns depend on distinct sets of signals that feed into a common pathway for organization of the bud site (CHANT and PRINGLE 1995). This model is complicated by the observation that at least one of the potential axial markers, Bud3p, is expressed in both haploid and **a**/α diploid cells, and elimination of Bud3p (or of Bud4p or Axl1p) results in a bipolar budding pattern. The model further invokes the presence of a haploid-specific gene product that can utilize the spatial pattern of Bud3p (and perhaps Bud4p) to generate the axial budding pattern (CHANT *et al.* 1995; CHANT and PRINGLE 1995). CHANT and PRINGLE (1995) suggest that a similar arrangement might exist for bipolar budding, although they point out that there are inherent differences in the placement of adjacent bud sites for axial *vs.* bipolar budding, suggestive of a transient signal for axial budding and more permanent signals for bipolar budding. If this is indeed the case, then the diploid-specific randomization of budding in *sec3* and related mutants might be due to an inability to properly organize or maintain the signal necessary for bipolar budding. Axial budding may remain unaffected because the axial marker localizes via an independent mechanism, *e.g.,* by the assembly of Bud3p, and perhaps other molecules, on the existing network of 10-nm filaments at the bud neck (see HAARER and PRINGLE 1987; KIM *et al.* 1991; CHANT *et al.* 1995). The random budding of profilin null mutants (HAARER *et al.* 1990) is likely due to the inability to properly organize even these axial marker proteins at the cell surface. That *sec1, 2, 6, 7,* or *18* mutants show normal bipolar budding suggests that budding polarity defects are not a general phenomenon of perturbing the secretory pathway. Thus, it is likely that Sec3p may be providing specific targeting information for localized secretion, perhaps through interactions with signaling molecules (*e.g.,* the adenylate cyclase complex) or with the actin cytoskeleton.

Conclusion: As more data become available, it is becoming increasingly apparent that cells can no longer be viewed as assemblages of independent pathways. Rather, the emerging picture is one in which virtually every function within the cell is subject to myriad interactions, receiving and sending signals via many "pathways" at all times. This view is especially apparent in the case of the actin cytoskeleton. As demonstrated in this study and in many others (see *e.g.,* BRETSCHER *et al.* 1994; WELCH *et al.* 1994; AMBERG *et al.* 1995; and references therein), actin function can be closely linked with normal secretory functions, cell polarity, osmotic

regulation, and nutrient sensing. In particular, it is now clear that there is a tight codependence of actin cytoskeleton organization and function with proteins of the secretory and endocytic pathways to maintain proper cell polarity and the normal integrity of cell growth.

We thank KATHLEEN CORRADO for providing the blot of yeast chromosomes; LINDA RILES and MAYNARD OLSON for providing blots of yeast cosmid library clones and subsequent mapping information; and A. ADAMS, A. BENDER, D. BOTSTEIN, C. CHAN, J. COOPER, D. DRUBIN, J. GERST, M. GUSTIN, J. FIELD, C. KAISER, S. LILLIE, P. NOVICK, S. PALMIERI, J. PRINGLE, H. RIEZMAN, M. TIBBETTS, K. WERTMAN and M. WIGLER for providing yeast strains and plasmids, and for helpful discussions. We also thank P. NOVICK for communicating results before publication, and the editor and reviewers for helpful comments. This work was supported by grants from the National Institutes of Health (NIH) to S.S.B and P.A.S., the American Cancer Society to S.S.B., and the National Science Foundation and the University of Texas Institute for Cellular and Molecular Biology to B.K.H., and by postdoctoral stipends from the NIH to B.K.H. and A.H.C. and The University of Michigan NIH Training Grant in Developmental Biology to B.K.H. This investigation was also supported in part by NIH grant MO1 RR-00042 to the Clinical Research Center of The University of Michigan.

LITERATURE CITED

ADAMS, A. E. M., and J. R. PRINGLE, 1984 Relationship of actin and tubulin distribution to bud growth in wild-type and morphogenetic-mutant *Saccharomyces cerevisiae*. J. Cell Biol. **98:** 934–945.

AMBERG, D. C., E. BASART and D. BOTSTEIN, 1995 Defining protein interactions with yeast actin *in vivo*. Nature Struc. Biol. **2:** 28–35.

BALASUBRAMANIAN, M. K., B. R. HIRANI, J. D. BURKE and K. L. GOULD, 1994 The *Schizosaccharomyces pombe cdc3*$^{+}$ gene encodes a profilin essential for cytokinesis. J. Cell Biol. **125:** 1289–1301.

BAUER, F., M. URDACI, M. AIGLE and M. CROUZET, 1993 Alteration of a yeast SH3 protein leads to conditional viability with defects in cytoskeletal and budding patterns. Mol. Cell. Biol. **13:** 5070–5084.

BENDER, A., and J. R. PRINGLE, 1991 Use of a screen for synthetic lethal and multicopy suppressee mutants to identify two new genes involved in morphogenesis in *Saccharomyces cerevisiae*. Mol. Cell. Biol. **11:** 1295–1305.

BÉNÉDETTI, H., S. RATHS, F. CRAUSAZ and H. RIEZMAN, 1994 The *END3* gene encodes a protein that is required for the internalization step of endocytosis and for actin cytoskeleton organization in yeast. Mol. Biol. Cell **5:** 1023–1037.

BRETSCHER, A., B. DREES, E. HARSAY, D. SCHOTT and T. WANG, 1994 What are the basic functions of microfilaments? Insights from studies in budding yeast. J. Cell Biol. **126:** 821–825.

CHANT, J., 1994 Cell polarity in yeast. Trends Genet. **10:** 328–333.

CHANT, J., and I. HERSKOWITZ, 1991 Genetic control of bud site selection in yeast by a set of gene products that constitute a morhogenetic pathway. Cell **65:** 1203–1212.

CHANT, J., and J. R. PRINGLE 1991 Budding and cell polarity in *Saccharomyces cerevisiae*. Curr. Opin. Gen. Dev. **1:** 342–350.

CHANT, J., and J. R. PRINGLE 1994 Patterns of bud-site selection in the yeast *Saccharomyces cerevisiae*. J. Cell Biol. **129:** 751–765.

CHANT, J., M. MISCHKE, E. MITCHELL, I. HERSKOWITZ and J. R. PRINGLE, 1995 Role of Bud3p in producing the axial budding pattern of yeast. J. Cell Biol. **129:** 767–778.

CHOWDHURY, S., K. W. SMITH and M. C. GUSTIN, 1992 Osmotic stress and the yeast cytoskeleton: phenotype-specific suppression of an actin mutation. J. Cell Biol. **118:** 561–571.

COSSART, P., 1995 Actin-based bacterial motility. Curr. Opin. Cell Biol. **7:** 94–101.

DEVEREUX, J., P. HAEBERLI and O. SMITHIES, 1984 A comprehensive set of sequence analysis programs for the VAX. Nucleic Acids Res. **12:** 387–395.

FLICK, J. S., and J. THORNER, 1993 Genetic and biochemical characterization of a phosphatidylinositol-specific phospholipase C in *Saccharomyces cerevisiae*. Mol. Cell. Biol. **13:** 5861–5876.

FREEMAN, N. L., Z. CHEN, J. HORENSTEIN, A. WEBER and J. FIELD, 1995 An actin monomer binding activity localizes to the carboxyl-terminal half of the *Saccharomyces cerevisiae* cyclase-associated protein. J. Biol. Chem. **270:** 5680–5685.

FUJITA, A., C. OKA, Y. ARIKAWA, T. KATAGAI, A. TONOUCHI *et al.*, 1994 A yeast gene necessary for bud-site selection encodes a protein similar to insulin-degrading enzymes. Nature **372:** 567–570.

GERST, J. E., K. FERGUSON, A. VOJTEK, M. WIGLER and J. FIELD, 1991 CAP is a bifunctional component of the *Saccharomyces cerevisiae* adenylyl cyclase complex. Mol. Cell. Biol. **11:** 1248–1257.

GERST, J. E., L. RODGERS, M. RIGGS and M. WIGLER, 1992 *SNC1*, a yeast homolog of the synaptic vesicle-associated membrane protein/sybnaptobrevin gene family: genetic interactions with the *RAS* and *CAP* genes. Proc. Natl. Acad. Sci. USA **89:** 4338–4342.

GOVINDAN, B., R. BOWSER and P. NOVICK, 1995 The role of Myo2, a yeast class V myosin, in vesicular transport. J. Cell Biol. **128:** 1055–1068.

GRUNDMANN, U., C. NERLICH, T. REIN, F. LOTTSPEICH and H. A. KÜPPER, 1988 Isolation of a cDNA coding for the placental protein 15 (PP15). Nucleic Acids Res. **16:** 4721.

HAARER, B. K., and S. S. BROWN, 1990 Structure and function of profilin. Cell Motil. Cytoskel. **17:** 71–74.

HAARER, B. K., S. H. LILLIE, A. E. M. ADAMS, V. MAGDOLEN, W. BANDLOW *et al.*, 1990 Purification of profilin from *Saccharomyces cerevisiae* and analysis of profilin-deficient cells. J. Cell Biol. **110:** 105–114.

HAARER, B. K., and J. R. PRINGLE, 1987 Immunofluorescence localization of the *Saccharomyces cerevisiae CDC12* gene product to the vicinity of the 10-nm filaments in the mother-bud neck. Mol. Cell. Biol. **7:** 3678–3687.

HAARER, B. K., A. S. PETZOLD and S. S. BROWN, 1993 Mutational analysis of yeast profilin. Mol. Cell. Biol. **13:** 7864–7873.

HAUGWITZ, M., A. A. NOEGEL, J. KARAKESISOGLOU and M. SCHLEICHER, 1994 *Dictyostelium* amoebae that lack G-actin-sequestering profilins show defects in F-actin content, cytokinesis, and development. Cell **79:** 303–314.

HOLTZMAN, D. A., S. YANG and D. G. DRUBIN, 1993 Synthetic-lethal interactions identify two novel genes, *SLA1* and *SLA2*, that control membrane cytoskeleton assembly in *Saccharomyces cerevisiae*. J. Cell Biol. **122:** 635–644.

KILMARTIN, J. V., and A. E. M. ADAMS, 1984 Structural rearrangements of tubulin and actin during the cell cycle of the yeast *Saccharomyces*. J. Cell Biol. **98:** 922–933.

LEW, D. J., and S. I. REED, 1993 Morphogenesis in the yeast cell cycle: regulation by Cdc28 and cyclins. J. Cell Biol. **120:** 1305–1320.

LEW, D. J., and S. I. REED, 1995 A cell cycle checkpoint monitors cell morphogenesis in budding yeast. J. Cell Biol. **129:** 739–749.

LILLIE, S. H., and S. S. BROWN, 1992 Suppression of a myosin defect by a kinesin-related gene. Nature **356:** 358–361.

LILLIE, S. H., and S. S. BROWN, 1994 Immunofluorescence localization of the unconventional myosin, Myo2p, and putative kinesin-related protein, Smy1p, to the same regions of polarized growth in *Saccharomyces cerevisiae*. J. Cell Biol. **125:** 825–842.

LILLIE, S. H., and J. R. PRINGLE, 1980 Reserve carbohydrate metabolism in *Saccharomyces cerevisiae:* responses to nutrient limitation. J. Bacteriol. **143:** 1384–1394.

LUPAS, A., M. VAN DYKE and J. STOCK, 1991 Predicting coiled coils from protein sequences. Science **252:** 1162–1164.

MA, H., S. KUNES, P. SCHATZ and D. BOTSTEIN, 1987 Plasmid construction by homologous recombination in yeast. Gene **58:** 201–216.

MACHESKY, L. M., S. J. ATKINSON, D. AMPE, J. VANDEKERCKHOVE and T. D. POLLARD, 1994 Purification of a cortical complex containing two unconventional actins from *Acanthamoeba* by affinity chromatography on profilin-agarose. J. Cell Biol. **127:** 107–115.

MAGDOLEN, V., D. G. DRUBIN, G. MAGES and W. BANDLOW, 1993 High levels of profilin suppress the lethality caused by overproduction of actin in yeast cells. FEBS Lett. **316:** 41–47.

MOORE, M. S., and G. BLOBEL, 1994 Purification of a Ran-interacting protein that is required for protein import into the nucleus. Proc. Natl. Acad. Sci. USA **91:** 10212–10216.

MUNN, A. L., B. J. STEVENSON, M. I. GELI and H. RIEZMAN, 1995 *end5, end6,* and *end7:* mutations that cause actin delocalization

and block the internalization step of endocytosis in *Saccharomyces cerevisiae*. Mol. Biol. Cell **6:** 1721–1742.

NA, S., M. HINCAPIE, J. H. MCCUSKER and J. E. HABER, 1995 *MOP2* (*SLA2*) affects the abundance of the plasma membrane H^+-ATPase of *Saccharomyces cerevisiae*. J. Biol. Chem. **270:** 6815–6823.

NOVICK, P., and D. BOTSTEIN, 1985 Phenotypic analysis of temperature-sensitive yeast actin mutants. Cell **40:** 415–426.

NOVICK, P., C. FIELD and R. SCHEKMAN, 1980 Identification of 23 complementation groups required for post-translational events in the yeast secretory pathway. Cell **21:** 205–215.

NOVICK, P., S. FERRO and R. SCHEKMAN, 1981 Order of events in the yeast secretory pathway. Cell **25:** 461–469.

PANTOLONI, D., and M.-F. CARLIER, 1993 How profilin promotes actin filament assembly in the presence of thymosin $\beta 4$. Cell **75:** 1007–1014.

PRINGLE, J. R., R. A. PRESTON, A. E. M. ADAMS, T. STEARNS, D. G. DRUBIN *et al.*, 1989 Fluorescence microscopy methods for yeast. Methods Cell Biol. **31:** 357–435.

PROTOPOPOV, V., B. GOVINDAN, P. NOVICK and J. E. GERST, 1993 Homologs of the synaptobrevin/VAMP family of synaptic vesicle proteins function on the late secretory pathway in *S. cerevisiae*. Cell **74:** 855–861.

ROTHSTEIN, R., 1991 Targeting, disruption, replacement, and allele rescue: integrative DNA transformation in yeast. Methods Enzymol. **194:** 281–301.

SAMBROOK, J., E. F. FRITSCH and T. MANIATIS, 1989 *Molecular Cloning: A Laboratory Manual*, Ed. 2. Cold Spring Harbor Laboratory Press, Cold Spring Harbor, NY.

SANGER, F., S. NICKLIN and A. R. COULSON, 1977 DNA sequencing with chain-terminating inhibitors. Proc. Natl. Acad. Sci. USA **74:** 5463–5467.

SHERMAN, F., G. R. FINK and J. B. HICKS, 1986 *Methods in Yeast Genetics*. Cold Spring Harbor Laboratory, Cold Spring Harbor, NY.

SIVADON, P., F. BAUER, M. AIGLE and M. CROUZET, 1995 Actin cytoskeleton and budding pattern are altered in the yeast *rvs161* mutant: the Rvs161 protein shares common domains with the brain protein amphiphysin. Mol. Gen. Genet. **246:** 485–495.

SOHN, R. H., and P. J. GOLDSCHMIDT-CLERMONT, 1994 Profilin: at the crossroads of signal transduction and the actin cytoskeleton. BioEssays **16:** 465–472.

VOJTEK, A., B. HAARER, J. FIELD, J. GERST, T. D. POLLARD *et al.*, 1991 Evidence for a functional link between profilin and CAP in the yeast *S. cerevisiae*. Cell **66:** 497–505.

WELCH, M. D., D. A. HOLTZMAN and D. G. DRUBIN, 1994 The yeast actin cytoskeleton. Curr. Opin. Cell Biol. **6:** 110–119.

Communicating editor: E. JONES